ARTICLE NO. 80-4010

C80-019

Use of Multiblade Coordinates for Helicopter Flap-Lag Stability with Dynamic Inflow

00001
00019
20009

Gopal H. Gaonkar*
India Institute of Science, Bangalore, India
and
David A. Peters†
Washington University, St. Louis, Mo.

Rotor flap-lag stability in forward flight is studied with and without dynamic inflow feedback via a multiblade coordinate transformation (MCT). The algebra of MCT is found to be so involved that it requires checking the final equations by independent means. Accordingly, an assessment of three derivation methods is given. Numerical results are presented for three- and four-bladed rotors up to an advance ratio of 0.5. While the constant-coefficient approximation under trimmed conditions is satisfactory for low-frequency modes, it is not satisfactory for high-frequency modes or for untrimmed conditions. The advantages of multiblade coordinates are pronounced when the blades are coupled by dynamic inflow.

Nomenclature

a	= slope of lift curve, rad^{-1} = 2π
C_{d_0}	= blade profile drag coefficient
C_L	= harmonic perturbation of roll moment
C_M	= harmonic perturbation of pitch moment coefficient
C_T	= harmonic perturbation of thrust coefficient (in figures also refers to steady value of thrust coefficient)
$\bar{f}$	= helicopter flat plate drag area/πR^2
F_{β_K}	= dimensionless force per unit length, perpendicular to blade and also to direction of rotation
k_m, k_I	= dimensionless apparent mass and inertia of an impermeable disk
m	= number of degrees of freedom per blade
M_k	= unsteady moment component from the kth blade at the rotor hub
n	= number of degrees of freedom of system
N	= number of blades
$N(\psi)$	= inflow coupling matrix, Eq. (6)
p	= dimensionless rotating flapping frequency = $\sqrt{1+\omega_\beta^2}$
P_k	= flapping stiffness of kth blade
r	= radial distance
R	= rotor radius
T_k	= unsteady thrust component from the kth blade at the rotor hub
$\bar{v}$	= dynamic inflow parameter, Eq. (3)
$\{X\}$	= vector of state variables, Eq. (5)
$\{U\}$	= vector of inflow parameters, Eq. (5)
Z_k	= stiffness parameter (equal to zero for zero elastic coupling or $\theta_k = 0$)
$\beta_k(\zeta_k)$	= perturbation flapping (lead-lag) angle of the kth blade
$\bar{\beta}_k$	= equilibrium flapping angle
$\beta(\zeta)$	= flapping (lead-lag) coordinate
β_{pc}	= precone angle
γ	= blade lock number
η	= real portion of lead-lag eigenvalue or lead-lag damping
θ_k	= pitch angle of the kth blade, $\bar{\theta}_k + \theta_\beta(\beta_k - \beta_{pc}) + \theta_\zeta \zeta_k$
$\bar{\theta}_k$	= equilibrium pitch angle of the kth blade, $\theta_0 + \theta_I \cos\psi_k + \theta_{II} \sin\psi_k + \theta_\beta(\bar{\beta}_k - \beta_{pc}) + \theta_\zeta \zeta_k$
$\theta_\beta, \theta_\zeta$	= pitch-flap and pitch-lag coupling ratios
λ	= steady inflow ratio (= ¼ ϕ)
μ	= rotor advance ratio
ν	= inflow perturbation
ν_0, ν_I, ν_{II}	= uniform, longitudinal, and lateral components of induced flow
$\bar{\nu}$	= induced inflow due to steady rotor thrust
ρ	= air density
σ	= rotor solidity
ψ	= azimuth position, dimensionless time
ψ_k	= azimuth position of the kth blade
$\omega_\beta, \omega_\zeta$	= dimensionless rotating flapping frequency
Ω	= rotor angular speed
{ }	= vector
[ ]	= matrix
$(\dot{\cdot})$	= $\dfrac{d}{d\psi}$

Received Jan. 29, 1979; revision received June 1, 1979.

Index categories: Helicopters; Aerodynamics; Nonsteady Aerodynamics.

*Professor. Associate Fellow AIAA.
†Associate Professor. Associate Fellow AIAA.

Introduction

IN multiblade coordinate transformation (MCT) individual blade deflections are represented by a finite Fourier series in the azimuth angle. The coefficients of this series are nonrotating blade coordinates which describe overall rotor motions. MCT provides a natural reference frame for rotor equations because perturbations due to the dynamic wake, fuselage, or active controls couple with the rotor motion in the form of nonrotating feedback effects. An N-bladed rotor, each blade having m degrees of freedom, is described exactly by Nm multiblade coordinates; each deflection is expressed via N multiblade coordinates: collective, differential (only for N even), and first-, second-, and higher-order longitudinal and lateral cyclic components. For rotors with an even number of blades, the differential component remains in the rotating system, but is reactionless for $N>2$ and does not directly couple with nonrotating feedback. In an approximate transformation, fewer than N multiblade coordinates are used, usually the two first-order cyclic components. Another noteworthy feature of MCT is the related constant-coefficient approximation. For rotors with polar symmetry, the periodic terms in the multiblade representation are not as influential as those in the individual blade representation. This is because MCT removes all harmonics save for integer multiples of N (for N odd) or of $N/2$ (for N even). Therefore, the constant coefficient approximation is greatly improved by the MCT.

An exact formulation via MCT with and without periodic terms was initiated by Hohenemser and Yin[1] and was applied to the problem of rigid flapping with feedback and elastic rotor support. It was indicated that MCT provides a viable method of obtaining the constant-coefficient approximation, a comprehensive study of which is due to Biggers.[2] Relevant to the present study, two conclusions from Biggers'[2] study should be mentioned: 1) omitting harmonic terms in blade coordinate equations provides useful approximations to low-frequency flapping modes up to an advance ratio of 0.5, although with high-frequency modes it should be used cautiously; 2) in the parametric region (frequency an integer multiple of ½ per rev) blade coordinate equations are still valid, but harmonic terms can not be neglected. Concerning the use of MCT in conjunction with nonrotating feedback effects, a recent study by Ormiston[3] shows appreciable effects of the dynamic wake on the flapping eigenvalues.

When individual blades have more than one degree of freedom, the algebra with MCT is not insignificant. In this context, Refs. 4 and 5 should be mentioned, in which blades having more than one degree of freedom are analyzed with MCT. The torsion-flap problem with active feedback controls is treated in Ref. 4 with respect to improving stability limits and gust response excursions; the flap-lag problem without feedback is treated in Ref. 5 with respect to the constant-parameter approximation. The results of Ref. 5 are somewhat encouraging, but are not comprehensive enough to draw any general conclusions. Furthermore, an anomaly[5] merits further study, which concerns different damping levels in the complete multiblade coordinate equations (all harmonic terms are included) when there are not interblade coupling effects. The algebraic aspects of MCT are not touched upon in Refs. 4 and 5.

The present paper is advanced over the preceding studies in several aspects:

1) It considers dynamic wake effects on flap-lag stability. The wake model of Ref. 6, which was used in earlier flap dynamics analyses,[3] is adapted here to include additional lead-lag degrees of freedom. This inflow model has the benefit of test results[3] and is suitable for low-frequency dynamic analysis.

2) It contains broad combinations of system parameters, wake parameters, and flight conditions, and compares three- and four-bladed rotors as to the applicability of the constant parameter approximation. Such a detailed study is warranted since damping levels in general are sensitive to trimming conditions, parameter combinations, and frequency content in response modes. It is mentioned in passing that, according to Ref. 7, parametric regions (in which harmonic terms should be retained) are not significant for the range studied here.

3) It includes a formal analytical treatment together with numerical results concerning an anomaly referred to earlier. It is shown that MCT has no effect on damping levels since it acts like a similarity transformation.

4) It shows that the manual computation of MCT algebra is not a feasible approach except for highly simplified models, and includes a comparative assessment of three methods for effecting MCT with regard to algebraic simplicity, computer time, and checking the final equations in multiblade coordinates.

Dynamic Inflow

The inflow model of Ref. 6 is adapted here to the case of flap-lag motions. It is based on the unsteady momentum theory and is applicable to the present low-frequency dynamic analysis. The assumption is that the inflow perturbation ν can be described as exhibiting basically three degrees of freedom: a uniform or collective component ν_0, and longitudinal and lateral cyclic components ν_I abd ν_{II}. The perturbation is with respect to the steady or trim value λ, where $4/3\ \lambda$ defines the trim inflow parameter ϕ. The variation of ν at a point r/R and azimuth position ψ is assumed to be of the form:

$$\nu=\nu_0+\nu_I(r/R)\cos\psi+\nu_{II}(r/R)\sin\psi \tag{1}$$

The dynamic inflow plays the role of a feedback system because perturbations in thrust induce perturbations in inflow which, in turn, affect thrust. Such a feedback mechanism is typified by the equations

$$\begin{bmatrix} k_m & 0 & 0 \\ 0 & -k_I & 0 \\ 0 & 0 & -k_I \end{bmatrix}\begin{Bmatrix} \dot\nu_0 \\ \dot\nu_0 \\ \dot\nu_{II}\end{Bmatrix}$$

$$=\begin{bmatrix} -2v & 0 & 0 \\ 0 & v/2 & 0 \\ 0 & 0 & v/2 \end{bmatrix}\begin{Bmatrix} \nu_0 \\ \nu_I \\ \nu_{II}\end{Bmatrix}+\begin{Bmatrix} C_T \\ C_M \\ C_L\end{Bmatrix}_{\text{aero}} \tag{2}$$

where the subscript "aero" in the extreme right-hand side vector indicates that the C_T, C_M, and C_L are from aerodynamic contributions only, where C_T, C_M, and C_L are coefficients of unsteady thrust, pitching, and rolling moments. The inflow parameter is governed by the relation

$$v=\frac{\mu^2+\lambda(\lambda+\bar\nu)}{(\mu^2+\lambda^2)^{1/2}} \tag{3}$$

where λ is the steady inflow ratio, and $\bar\nu$ is the induced portion of the inflow due to steady rotor thrust. The time constant is equal to $0.4244/v$ for ν_0 and to $0.2264/v$ for ν_I and ν_{II}. The elements of the mass matrix k_m and k_I, are not known for actual conditions. As approximations, these elements are evaluated from the potential flow around a solid disk for which $k_m=8/3\pi$ and $k_I=16/45\pi$.

The expressions for C_T, C_M, and C_L are cumbersome for a multiblade flap-lag system with dynamic inflow. They are not reproduced here. Rather, a brief account of the derivations of these three coefficients is sketched in the sequel to provide a qualitative understanding between in-plane dynamics and inflow perturbations.

$$C_T=\frac{1}{(\rho\pi\Omega^2R^4)}\sum_{k=1}^{N}T_k=\left[\frac{a\sigma}{\gamma}\cdot\frac{1}{N}\sum_{k=1}^{N}\int_0^1\bar F_{\beta_k}\,\mathrm{d}\bar r\right]_{\text{unsteady}} \tag{4a}$$

$$C_M=-\frac{a\sigma}{\gamma}\cdot\frac{1}{N}\cdot\sum_{k=1}^{N}(\ddot\beta_k+P_k\beta_k+2\bar\beta_k\dot\zeta_k+Z_k\zeta_k)\cos\psi_k \tag{4b}$$

$$C_L=-\frac{a\sigma}{\gamma}\cdot\frac{1}{N}\cdot\sum_{k=1}^{N}(\ddot\beta_k+P_k\beta_k+2\bar\beta_k\dot\zeta_k+Z_k\zeta_k)\sin\psi_k \tag{4c}$$

The subscript "unsteady" indicates that the perturbed or unsteady component is applicable. Expressions for $\bar F_{\beta_k}$ are given in Ref. 7 in terms of the θ_k, λ, β_k, $\dot\beta_k$, ζ_k, and $\dot\zeta_k$. However, in Ref. 7, $\bar F_{\beta_k}$ is evaluated on the basis of the steady component of λ only, whereas the present study considers the steady component λ on which is superimposed the unsteady or the inflow perturbation ν defined by Eq. (1). It should be emphasized that the ζ and $\dot{\zeta}$ terms are not negligible for evaluation of C_T, C_M, and C_L.

For the purpose of further discussion, Eq. (2) will be symbolically represented in the state variable form:

$$\{\dot{U}\} = [A_2]_{3\times 4N}\{X\} + [A_3]_{3\times 3}\{U\} \tag{5}$$

where U is the 3×1 vector with components ν_0, ν_I, and ν_{II}, and X is the $4N\times 1$ vector with components $\beta_1, \dot{\beta}_1, \ldots \beta_N$, $\dot{\beta}_N$, $\zeta_1, \ldots \zeta_N$, and $\dot{\zeta}_N$.

The equations of flap-lag motions as given in Ref. 7 are extended here to the case of dynamic inflow. The $4N\times 1$ flap-lag vector X introduced in Eq. (5) has the representation

$$\dot{X} = \underset{4N\times 4N}{[A(\psi)]X} + \underset{4N\times 3}{[N(\psi)]U} \tag{6}$$

The elements of matrix $A(\psi)$ are generated from Ref. 7. For a typical kth blade, $N(\psi_k)$ is the 4×3 matrix given in Table 1. Eqs. (5) and (6), when combined, have the state representation

$$\begin{Bmatrix} \dot{X} \\ \\ \dot{U} \end{Bmatrix} = \begin{bmatrix} A(\psi) & N(\psi) \\ \\ A_2(\psi) & A_3 \end{bmatrix} \begin{Bmatrix} X \\ \\ U \end{Bmatrix} \tag{7}$$

or in a compact form

$$\dot{Z} = D(\psi)Z \tag{8}$$

where Z is the $(4N+3)\times 1$ composite state vector and $D(\psi)$ is the $(4N+3) \times (4N+3)$ composite state matrix.

Multiblade Coordinate Transformation

MCT expresses original blade equations in a rotating frame of reference in terms of multiblade coordinates in a nonrotating frame. It is formulated here to assess its feasibility. Referring to the $4N\times 1$ vector X of Eq. (7), the transformation $4N\times 1$ multiblade coordinate vector Y is

$$\{X\} = [B(\psi)]\{Y\} \tag{9}$$

where $B(\psi)$ is the $4N\times 4N$ periodic matrix which has closed-form inverse and derivative matrices.[8] The algebraic structure of B is better revealed by expressing Eq. (9) in an equivalent form:

$$\{X\} = \begin{bmatrix} M(\psi) & 0 \\ \\ 0 & M(\psi) \end{bmatrix} \{Y\} \tag{10}$$

where $Y^T = [\beta_0, \dot{\beta}_0, \beta_d, \dot{\beta}_d, \beta_I, \dot{\beta}_I, \beta_{II}, \dot{\beta}_{II}, \ldots \zeta_0, \dot{\zeta}_0, \zeta_d, \dot{\zeta}_d, \zeta_I, \dot{\zeta}_I \ldots \zeta_N, \dot{\zeta}_N]$ and where $M(\psi)$, which is referred to here as the basic $2N\times 2N$ MCT matrix, is given in Table 2. The third column in $M(\psi)$, with typical element $(-1)^k$, refers to the differential modes β_d and ζ_d which are applicable for the case N even only.

When X in Eq. (7) is written in terms of Eq. (9), the state equation in multiblade coordinates is

$$\begin{Bmatrix} \dot{Y} \\ \\ \dot{U} \end{Bmatrix} = \begin{bmatrix} -B^{-1}\dot{B} + B^{-1}AB & N \\ \\ A_2B & A_3 \end{bmatrix} \begin{Bmatrix} Y \\ \\ U \end{Bmatrix} \tag{11}$$

or in compact form

$$\dot{Z} = F(\psi)Z \tag{12}$$

In general, the greater the number of blades, the better the accuracy of the constant coefficient approximation of Eq.

Table 1 Elements of $N(\psi)$

$$\frac{\gamma}{8}\begin{bmatrix} 0 & 0 & 0 \\ -(4/3+2\mu\sin\psi_k) & -(1+4/3\mu\sin\psi_k)\cos\psi_k & -(1+4/3\mu\sin\psi_k)\sin\psi_k \\ 0 & 0 & 0 \\ 3\phi - \bar{\theta}_k(4/3+2\mu\sin\psi_k) & 2\phi\cos\psi_k & 2\phi\sin\psi_k \\ \quad +4\mu\bar{\beta}_k\cos\psi_k & \quad -\bar{\theta}_k(1+4/3\mu\sin\psi_k)\cos\psi_k & \quad -\bar{\theta}_k(1+4/3\mu\sin\psi_k)\sin\psi_k \\ & \quad +8/3\mu\bar{\beta}_k\cos^2\psi_k & \quad +8/3\mu\bar{\beta}_k\sin\psi_k\cos\psi_k \end{bmatrix}$$

Table 2 Elements of $M(\psi)$

$$M(\psi) = \begin{bmatrix} 1 & 0 & -1 & 0 & C\psi_1 & 0 & S\psi_1 & 0 & \ldots & C(M\psi_1) & 0 & S(M\psi_1) & 0 \\ 0 & 1 & 0 & -1 & -S\psi_1 & C\psi_1 & C\psi_1 & S\psi_1 & \ldots & -MS(M\psi_1) & C(M\psi_1) & MC(M\psi_1) & S(M\psi_1) \\ \vdots & \vdots & \vdots & \vdots & \vdots & \vdots & \vdots & \vdots & & \vdots & \vdots & \vdots & \vdots \\ 1 & 0 & (-1)^k & 0 & C\psi_k & 0 & S\psi_k & 0 & \ldots & C(M\psi_k) & 0 & S(M\psi_k) & 0 \\ 0 & 1 & 0 & (-1)^k & -S\psi_k & C\psi_k & C\psi_k & S\psi_k & \ldots & -MC(M\psi_k) & C(M\psi_k) & MC(M\psi_k) & S(M\psi_k) \\ \vdots & \vdots & \vdots & \vdots & \vdots & \vdots & \vdots & \vdots & & \vdots & \vdots & \vdots & \vdots \\ 1 & 0 & (-1)^N & 0 & C\psi_N & 0 & S\psi_N & 0 & \ldots & C(M\psi_N) & 0 & S(M\psi_N) & 0 \\ 0 & 1 & 0 & (-1)^N & -S\psi_N & C\psi_N & C\psi_N & S\psi_N & \ldots & -MC(M\psi_N) & C(M\psi_N) & MC(M\psi_N) & S(M\psi_N) \end{bmatrix}$$

$M = N/2$ (N even), $M = (N-1)/2$ (N odd)

(12). Conventionally, algebra with Eq. (12) is carried out by hand with the use of identities such as

$$\sum_{k=1}^{N} \sin^2\psi_k = \frac{N}{2}$$

etc. However, the manual algebraic manipulations experienced in the present study merit further comment.

Several independent derivations of the operations in Eq. (12) had to be made by hand, each one requiring 70-100 pages of algebra. The results of each derivation had to be compared term by term to check for errors. Several iterations were required before a consistent set of equations could be obtained. Therefore, alternate methods were examined whereby the amount of hand algebra in the MCT could be reduced. Altogether, three methods of derivation were compared.

In the first method, Eq. (12) is treated completely digitally for each discrete value of the azimuth position. The inputs to the digital system are the closed-form expressions of periodic matrices A, B, B^{-1}, $\dot{B}$, N, and A_2. Observe that $B^{-1}\dot{B}$ and A_3 are constant matrices. The matrix operations indicated in Eq. (12) are executed by the computer. To obtain the constant-coefficient approximation, each element of the state matrix is averaged by a quadrature subroutine which is based on Simpson's rule. For comparable accuracy with the other two methods, a quadrature step size of $2\pi/50$ is required.

In the second method, the matrices $A(\psi)$, $B(\psi)$, $B^{-1}(\psi)$, $A_2(\psi)$, and $N(\psi)$ are expressed in Fourier series by hand ($B^{-1}\dot{B}$ and A_3 are constant coefficients). The crux of this process is to express $F(\psi)$ in Eq. (12) in the form

$$G_0 + G_{1c}\cos\psi + G_{1s}\sin\psi + G_{2c}\cos2\psi$$
$$+ G_{2s}\sin2\psi + G_{3c}\cos3\psi + G_{3s}\sin3\psi$$

where the G matrices are written explicitly in terms of multiplications of constant matrices. In this second method, computer and analyst share the algebra in that the analyst performs the Fourier algebra on a matrix level (as in the preceding), but the computer performs the arithmetic of matrix multiplications. The advantage over the first method is that the computer multiplications are required only once per problem rather than one per time increment. The constant-coefficient equations are obtained directly from G_0 (i.e., $\dot{Z} = G_0 Z$). The third method of obtaining the MCT is the original method,[1-5] in which all matrix multiplications are performed by hand. The constant-coefficient terms are then obtained by inspection.

For either method of performing the transform, some sort of numerical check is advisable. One simple check is to compare the damping as calculated from Eq. (8) with that calculated from Eq. (12). When all periodicity is retained, the two equations should give identical damping. This also implies that, when the blades are uncoupled, the multiblade equations should give N repeated values of the flap and lag damping. This is because the transformation in Eq. (9) merely modulates X by a periodic function. Thus, the frequency of Y can be shifted by integer multiples of 1/rev, but the decay of Y and X must be the same. For example, for a three-bladed rotor with no interblade coupling, the two sets of three differential equations in rotating and nonrotating frame must produce three pairs of eigenvalues with identical flap damping and another three pairs with identical lead-lag damping. A second check of the MCT is to examine the harmonics of $F(\psi)$. Only integer multiples of N per rev (for N odd) or $N/2$ per rev (for N even) should appear.

A distinct advantage of the first method is the simplicity and reliability of obtaining numerically a valid set of constant-coefficient equations in multiblade coordinates. The disadvantage is the excessive computer time which results from averaging of the periodic coefficients by numerical quadrature. However, the use of this first method for spot-checks in conjunction with either of the other two methods is found to be valuable. The third method has the advantage of providing constant parameter approximations in closed form as required in a qualitative study and, as expected, takes the least amount of computer time. However, the disadvantage is the horrendous manual algebra as mentioned earlier.

For a three-bladed rotor without dynamic inflow in multiblade coordinates, the third method takes 2.15 s to obtain the final eigenvalues, as compared with 5.33 and 74.4 s taken by the second and first methods, respectively. It can also be shown from algorithmic details that the second method always takes about 2.5 times the machine time of the third method. Therefore, only the third method is used to compare machine time between the constant-coefficient approximation and the exact analysis. There is, naturally, a significant saving in machine time with the constant-coefficient approximation, for which it is also relatively simpler to physically interpret eigenmode and frequency results. Without dynamic inflow, when a single-blade analysis is adequate, one has to compare 2.15 s (for the constant-coefficient approximation of a three-bladed rotor without dynamic inflow in multiblade coordinates) with 13.64 s (for the Floquet analysis from a single-blade model). However, it is equally instructive to compare the same 2.15 s with the 53.1 s that are required for the Floquet analysis of a three-bladed model without dynamic inflow. With the inclusion of dynamic inflow, for which a three-bladed model analysis is necessary, one has to compare 3.1 s with 106.9 s of Floquet analysis—a 35-fold savings. Although the preference of one method to the other two would depend upon such diverse factors as availability of manpower and economics of digital facilities, the second method is preferable for the type of models treated here ($12 \le n \le 20$) as a reasonable compromise between computer time and manual algebra.

Discussion of Results

Unless otherwise specified, all results shown are for the parameters: $p = 1.15$, $\omega_\zeta = 1.4$, $Z = 0$, $\gamma = 5$, $C_T = 0.01$, $C_{d_0} = 0.01$, $\sigma = 0.05$, $\bar{f} = 0$, trimmed. The first set of results, shown in Fig. 1, are damping plots for a three-bladed rotor without dynamic inflow. Several different damping values are plotted for the trimmed configuration ($\bar{\beta}_I = \bar{\beta}_{II} = 0$, cyclic flapping suppressed). Assumed parameter values are also identified in the same figure. The trimmed configuration is the case in which the cyclic pitch is adjusted at each advance ratio such that the steady portions of C_L and C_M are zero and that C_T remains constant with μ. This is accomplished by an approximate harmonic balance in which the inflow derivatives are assumed to be equal to pitch angle derivatives. For $\mu < 0.4$, the results are identical with the more exact trim formulas in Ref. 9. For $\mu > 0.4$, there is a 10-15% difference between the pitch angles used here and the more exact results of Ref. 9.

The first curve in Fig. 1, labeled "exact," is the result obtained from Floquet theory when all harmonic terms are retained. The result was calculated in four different ways: once from the original equations in a rotating frame, and once from each of the three derivations of the multiblade equations mentioned earlier. Each of the four analyses provided identical results, with each of the multiblade representations having two sets of three pairs of eigenvalues with repeated damping. It is interesting to compare these results with the similar curve calculated in Ref. 7. For $\mu < 0.3$ the two curves are identical. For $\mu > 0.3$, there is a small deviation due to both the small-angle assumption ($\sin\theta = \theta$, $\cos\theta = 1$ is used here, while $\sin\theta$ and $\cos\theta$ are retained in Ref. 7) and the approximate trim. It is also interesting to compare these results with similar calculations in Ref. 5. However, in Ref. 5, three separate damping curves are obtained from Floquet theory. One curve agrees with the present curve for $\mu < 0.3$, but the other two curves do not. It seems that some slight algebraic error must be present in the multiblade transformation of Ref. 5, since only one damping value is theoretically possible when there is no blade coupling.

Also in Fig. 1 the damping from the constant-coefficient approximation is shown. The different sets of multiblade equations give identical sets of constant-coefficient eigenvalues, but each set no longer has repeated damping. The collective mode (frequency ω_ζ) and the regressing mode (frequency $\omega_\zeta - 1$) show damping virtually identical to the exact Floquet solution. The progressing mode (frequency $\omega_\zeta + 1$), however, shows no improvement over the rotating, constant-coefficient equations. Thus, for this trimmed case, the multiblade coordinates can be used to eliminate periodic coefficients provided that the higher-frequency motions ($\omega_\zeta + 1$) are not required. The three constant-coefficient curves also agree with the constant-coefficient curves of Ref. 5, for $\mu < 0.3$. This implies that the error in Ref. 5 does not greatly affect the constant-coefficient terms.

The multiblade transformation has also been performed for a four-bladed rotor. The exact Floquet results are identical to the three-bladed results, because the blades are uncoupled. The constant-coefficient approximation is also identical to the three-bladed result for the collective, regressing, and progressing modes. The fourth mode for the four-bladed rotor is the scissor or the reactionless mode. For the constant-coefficient approximation, the reactionless mode gives the same damping as the single-blade constant-coefficient result in Fig. 1. The computing time for four blades is larger, however, than for three blades by a factor of 3/1. The effect of trimming the fuselage drag is shown in Fig. 2. The lead-lag mode is stabilized by the extra inflow. Despite the change in stability, however, the accuracy of the constant-coefficient approximation is the same as without fuselage drag.

Figure 3 shows similar comparison for the untrimmed rotor ($\theta_I = \theta_{II} = 0$, cyclic flapping present). Again, all four methods give identical damping when harmonic terms are retained; and this damping agrees with the similar calculation in Ref. 7. For the constant-coefficient approximations, however, only the collective mode has the correct damping. The regressing and progressing modes give considerably different damping, the latter being even worse than that for the rotating constant-coefficient approximation. Thus, for untrimmed conditions such as in tail rotors or wind turbines, the constant-coefficient approximation could not be used for

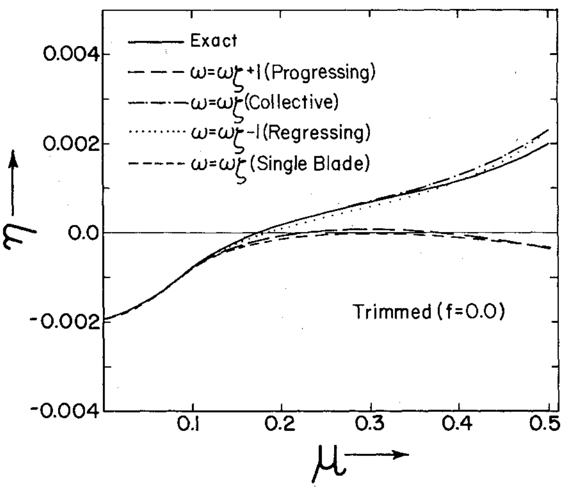

Fig. 1 Constant-coefficient approximation, baseline.

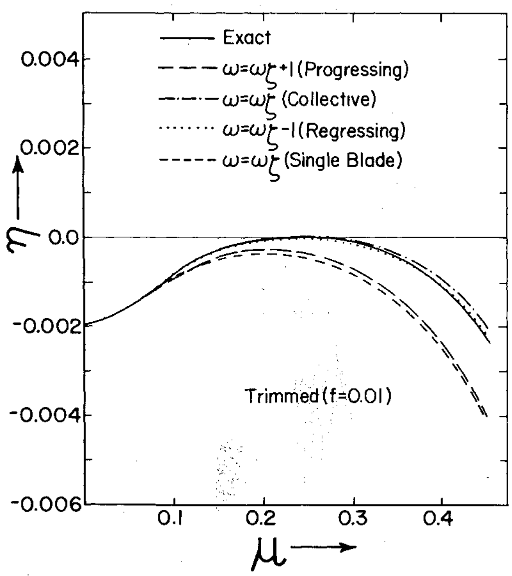

Fig. 2 Constant coefficient, $\bar{f} = 0.01$.

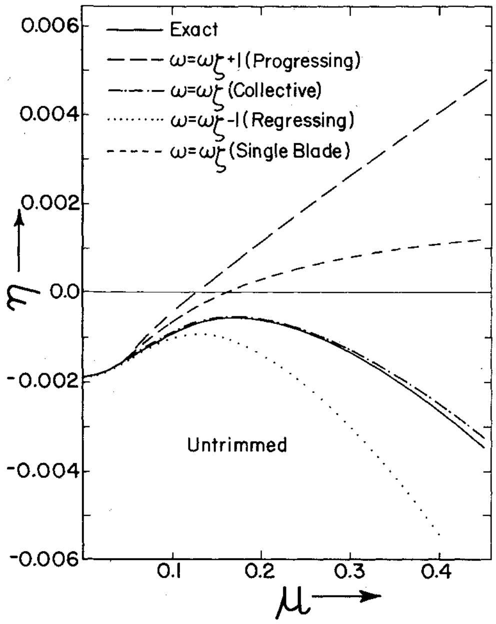

Fig. 3 Constant coefficient, untrimmed.

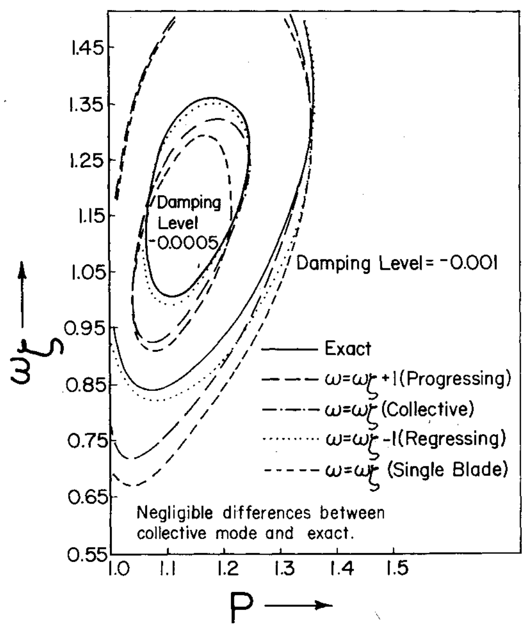

Fig. 4 Constant coefficient, $C_T = 0.005$, $\mu = 0.3$.

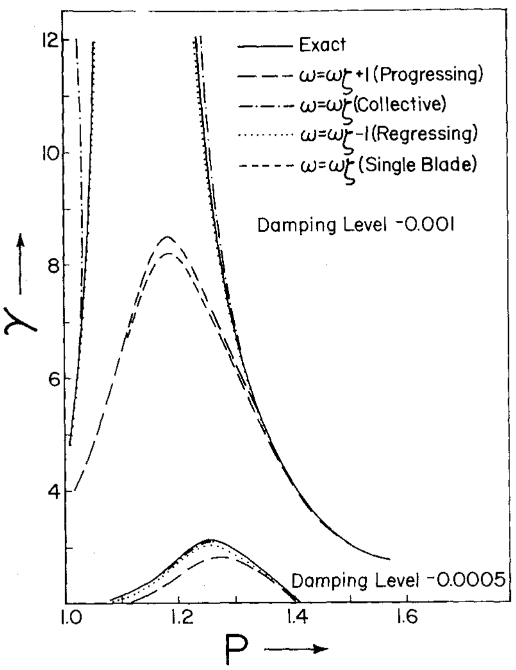

Fig. 5 Constant coefficient, $C_T = 0.005$, $\mu = 0.3$.

problems in the low-frequency ($\omega_\zeta - 1$) regimes (e.g., for rotor-support coupling) nor could it be used for problems in the high-frequency ($\omega_\zeta + 1$) regime.

The next step in the analysis is to determine if the preceding conclusions are valid for all realistic values of the blade parameters, (p, γ, ω_ζ, C_T), or if there are regions where the constant-coefficient approximation is greatly improved or greatly deteriorated with respect to previous results. It has already been shown in Ref. 7 that parametric regions are not significant for lag damping. Thus, the effect of blade parameters on the constant-coefficient approximation for in-plane damping should not be as pronounced as it is for flap damping.

The first comparisons are the contours of constant damping in the $p\omega_\zeta$ plane, Fig. 4. The contours are for $C_T/\sigma = 0.1$, for which no instabilities occur.[7] The exact contour from Floquet theory is compared with contours for each of the multiblade branches. The damping trends in the $p\omega_\zeta$ plane are not greatly affected by p or ω_ζ. The constant-coefficient results for both the single blade and for the progressing mode are slightly improved for stiff ω_ζ. The regressing and collective modes, however, give constant-coefficient damping that is virtually identical to the exact value. Thus, the accuracy of the constant-coefficient approximation is not dependent on C_T or ω_ζ.

The second comparison is given in Fig. 5 in the form of contours of constant damping in the $p\gamma$ plane. The parametric regions that are normally seen in flap damping in the $p\gamma$ plane (discontinuities in damping) are not found for these in-plane damping curves. As a result, the accuracy of the constant-coefficient approximation for the regressing and collective modes is maintained for all p and γ combinations. The single-blade and progressing mode approximations show improved accuracy at very high p or very low γ, although they are not accurate in the normal $p\gamma$ range.

The results to follow pertain to the effect of dynamic inflow on the lead-lag damping. With coupling due to dynamic inflow, it is no longer true that the periodic system must yield three repeated values of damping. The coupled equations may yield three different damping values. These are plotted in Fig. 6 for a stiff in-plane rotor. The analysis of Ref. 6 predicts that the effect of dynamic inflow should be largest for low μ and low frequency. Thus, one would expect the maximum effect to occur for the regressing mode at low advance ratio. This is

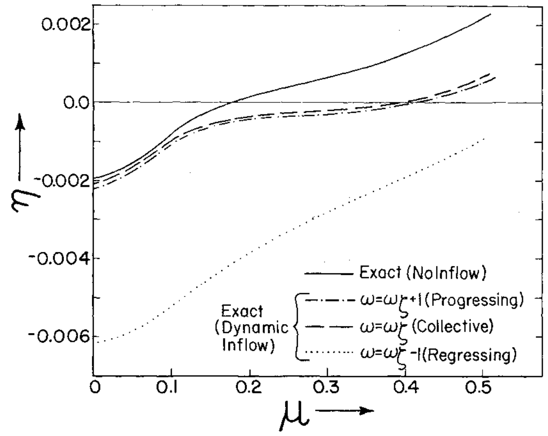

Fig. 6 Effect of dynamic inflow, $\omega_\zeta = 1.4$.

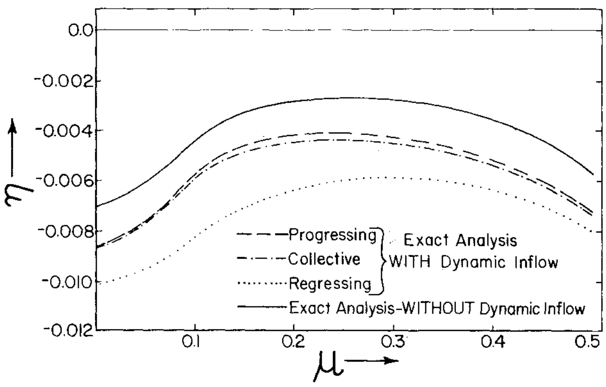

Fig. 7 Effect of dynamic inflow, $\omega_\zeta = 0.7$.

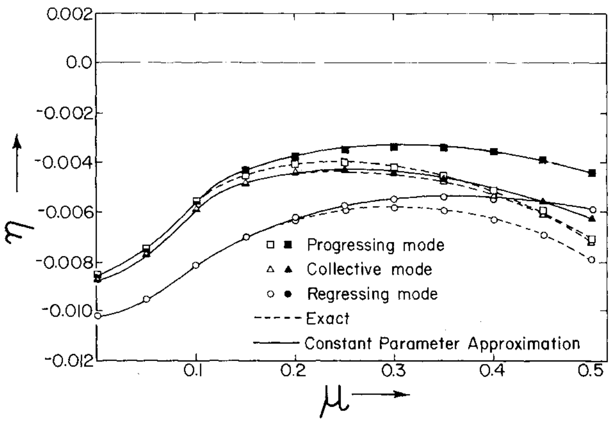

Fig. 8 Constant coefficient, dynamic inflow, $\omega_\zeta = 0.7$.

indeed the case. The results confirm the prediction of Ref. 6 that dynamic inflow can affect blade stability and, hence, air and ground resonance. The large increase in in-plane damping, of itself, should stabilize air and ground resonance. On the other hand, dynamic inflow also affects the helicopter stability derivatives,[6] and these could have an adverse effect on ground resonance. A surprising result in Fig. 6 is that, at high advance ratios, even the progressing mode damping is affected by dynamic inflow. This was not expected; but, in retrospect, it is clearly a result of the effect of time constant increasing with μ.

Figure 7 presents the effect of dynamic inflow for a soft in-plane rotor. The regressing mode is highly stabilized, and the trend is similar to that for the stiff in-plane rotor. This is to be expected since $|\omega_\zeta - 1|$ is about the same for $\omega_\zeta = 0.7$ and $\omega_\zeta = 1.4$. The collective and progressing modes for $\omega_\zeta = 0.7$, however, show a much larger effect of dynamic inflow at μ close to zero than do their counterparts for $\omega_\zeta = 1.4$. This is to be expected for the collective mode because the collective frequency at $\omega_\zeta = 0.7$ is only half of $\omega_\zeta = 1.4$, and it tends to couple more strongly with the low-frequency wake. The behavior of the progressing mode, however, is less easily explained when μ is close to zero. It would seem that the progressing mode for $\omega_\zeta = 0.7$ ($\omega = 1.7$) should behave as the collective mode for $\omega_\zeta = 1.4$. However, it must be remembered that the time constant for the collective mode is twice that of the cyclic mode. Thus, these two modes have different reactions to dynamic inflow at the same frequency.

The final set of results, shown in Fig. 8, gives a picture of the accuracy of the constant-coefficient approximation in the presence of dynamic inflow. As expected, the regressing and collective modes are well approximated up to $\mu = 0.4$; but the progressing mode requires the retention of harmonic terms. Thus, for problems of rotor-body coupling (trimmed rotors) with dynamic inflow, the multiblade coordinates provide satisfactory constant-coefficient representations. The accuracy of such representations offers promise for at least two reasons. First, the added complexities of Floquet theory (including the difficult task of interpreting frequencies) can be avoided. Second, computing time can be reduced. This saving is particularly significant for problems in which blade motions are coupled through fuselage motions, dynamic inflow, or rotor feedback. For an uncoupled rotor system, a three-bladed multiblade analysis with constant coefficients requires about 1/6 of the computing time of Floquet theory for a single blade. For a system with three coupled blades, however, the Floquet theory must be applied to all three blades. As a result, the constant-coefficient analysis with dynamic inflow in multiblade coordinates requires only about 3% of the computing time of Floquet theory. Therefore, the method of multiblade coordinates is most useful when blade motions are coupled.

Other data on flap damping are not reproduced here for brevity, since they essentially confirm the earlier findings of Biggers.[2] The only noteworthy feature is that flap damping is reduced with the inclusion of dynamic inflow.

Concluding Remarks

The method of obtaining multiblade equations is extended here with the suggested approach of computer-aided algebra with built-in checking procedures. The conventional approach involves a formidable amount of algebra and several iterations. It is shown that with the newly suggested approach it is possible to treat viable rotor models involving interblade coupling due to nonrotating feedback effects. A formal analytical treatment confirms the numerical data, which show that multiblade coordinate transformation is a similarity transformation in that damping levels from Floquet theory must yield identical results, whether they are in the rotating frame or in the nonrotating frame. It is further shown that the constant-coefficient approximation offers great promise for problems of rotor-body coupling with dynamic inflow under trimmed conditions. By comparison to Floquet theory, this approximation offers a marked reduction in machine time (of the order of 1 to 35 for a three-bladed rotor with inflow) and provides a much simpler way of interpreting frequencies and eigenmodes. The numerical results further demonstrate the following:

1) The constant-coefficient approximation in multiblade coordinates is accurate for the collective mode under all conditions; it is accurate for regressing mode only for trimmed conditions; and it is accurate for the progressing mode only at extremely large values of p or low values of γ.

2) The constant-coefficient results for the reactionless mode in a four-bladed rotor are identical to the constant-coefficient results for a single blade. But, these results are not accurate for $\mu > 0.2$.

3) Dynamic inflow is stabilizing for all in-plane modes and destabilizing for all flapping modes, but the most significant effect is for the lead-lag regressing mode at low advance ratios.

4) For analyses of uncoupled blades, the constant-coefficient multiblade approximation requires approximately 1/6 of the computing time of Floquet theory; but for coupled blade motions of a three-bladed rotor with dynamic inflow, it requires only 3% of the computing time of Floquet theory.

Acknowledgment

Assistance of D. Chen and A. K. Subramanian is appreciated. This research was supported in part by the Office of Research and Projects and Assistant Vice President of Special Programs and Minority Affairs of Southern Illinois University-Edwardsville, and in part by the National Science Foundation, NSF Grant ENG76-84439.

References

[1] Hohenemser, K.H. and Yin, S.K., "Some Applications of the Method of Multiblade Coordinates," *Journal of the American Helicopter Society*, Vol. 16, April 1971, pp. 3-12.

[2] Biggers, J.C., "Some Approximations to the Flapping Stability of Helicopter Rotors," *Journal of the American Helicopter Society*, Vol. 19, Oct. 1974, pp. 24-33.

[3] Ormiston, R.A., "Application of Simplified Inflow Models to Rotorcraft Dynamic Analysis," *Journal of the American Helicopter Society*, Vol. 21, July 1976, pp. 34-37.

[4] Gaonkar, G.H., Hohenemser, K.H., and Yin, S.K., "Random Gust Response Statistics for Coupled Torsion-Flap Blade Vibrations," *Journal of Aircraft*, Vol. 9, Oct. 1972, pp. 726-729.

[5] Kaza, K.R.V. and Hammond, C.E., "An Investigation of Flap-Lag Stability of Wind Turbine Rotors in the Presence of Velocity Gradients and Helicopter Rotors in Forward Flight," *Proceedings of the AIAA/ASME/SAE 17th Structures, Structural Dynamics, and Materials Conference*, Valley Forge, Pa., May 5-7, 1976, pp. 421-431.

[6] Peters, D.A., "Hingeless Rotor Frequency Response with Unsteady Inflow and Elastic Blade Bending," NASA SP-352, Feb. 1974, pp. 1-12.

[7] Peters, D.A., "Flap-Lag Stability of Helicopter Rotor Blades in Forward Flight," *Journal of the American Helicopter Society*, Vol. 20, Oct. 1975, pp. 2-13.

[8] Gaonkar, G.H., "A General Method with Shaping Filters to Study Random Vibration Statistics of Lifting Rotors with Feedback Controls," *Journal of Sound and Vibration*, Vol. 72, 1972, pp. 213-225.

[9] Wei, F.S. and Peters, D.A., "Lag Damping in Autorotation by a Perturbation Method," *Proceedings of the Annual Forum of the American Helicopter Society*, Paper 78-25, May 11-13, 1978.